

# A Fluorescence-Based Sensor Assay that Monitors General Protein Aggregation in Human Cells

Marisa Pereira, Diogo Tomé, Ana S. Domingues, Ana S. Varanda, Cristiana Paulo, Manuel A. S. Santos, and Ana R. Soares\*

Protein conformational disorders are characterized by disruption of protein folding and toxic accumulation of protein aggregates. Here we describe a sensitive and simple method to follow and monitor general protein aggregation in human cells. Heat shock protein 27 (HSP27) is an oligomeric small heat shock protein that binds and keeps unfolded proteins in a folding competent state. This high specificity of HSP27 for aggregated proteins can be explored to monitor aggregation in living cells by fusing it to a fluorescent protein as Green Fluorescent Protein (GFP). We have constructed a HeLa stable cell line expressing a HSP27:GFP chimeric reporter protein and after validation, this stable cell line is exposed to different agents that interfere with proteostasis, namely Arsenite, MG132, and A $\beta$ -peptide. Exposure to proteome destabilizers lead to re-localization of HSP27:GFP fluorescence to foci, confirming that our reporter system is functional and can be used to detect and follow protein aggregation in living cells. This reporter is a valuable tool to setup wide-genetic screens to identify genes and pathways involved in protein misfolding and aggregation.

## 1. Introduction

The accumulation of protein aggregates is a common feature of protein conformational disorders and is generally correlated with the onset of diseases, such as amyotrophic lateral sclerosis (ALS), Alzheimer's (AD), Parkinson's (PD), Huntington's (HD) disease, and other age-related diseases (ARD).<sup>[1–5]</sup> Aggregation of proteins like amyloid-beta peptide (A $\beta$ ),  $\alpha$ -synuclein ( $\alpha$ -syn), or huntingtin (Htt) is commonly found in AD, PD, and HD, respectively.<sup>[6–8]</sup> Aggregates of non-amyloid proteins are


associated with other protein misfolding diseases. For example, aggregation of superoxide dismutase 1 (SOD-1) is linked to ALS<sup>[9]</sup> and  $\alpha$ 1-antitrypsin mutants aggregate in the endoplasmic reticulum of hepatocytes leading to liver-disease onset.<sup>[10]</sup> Moreover, evidences in different animal models indicate that widespread protein aggregation increases with aging. In *Caenorhabditis elegans* *Caenorhabditis elegans* there is accumulation of several proteins through the lifespan, including homologs of protein aggregates found in AD and ALS.<sup>[11,12]</sup> In mice hearts multiple proteins also aggregate with age and are linked to AD,<sup>[13]</sup> whereas post-mortem healthy human-aged brains show abnormal accumulation of tau, A $\beta$ , and  $\alpha$ -syn inclusions.<sup>[14]</sup>

Different in vitro and in vivo protein misfolding/aggregation monitoring strategies have been developed in recent years.

Thioflavin (ThT) is a molecular probe that is commonly used to detect amyloid fibrils, in particular  $\beta$ -sheet-rich structures of amyloid.<sup>[15–17]</sup> Fluorescent reporter proteins (GFP, YFP) have been fused to the C- or N-terminus of target proteins, allowing monitoring the aggregation status of such proteins by microscopy or flow cytometry.<sup>[17]</sup> GFP fused to the C-terminus of A $\beta$ 40 and A $\beta$ 42 peptides is used to screen A $\beta$  mutant peptide libraries expressed in *Escherichia coli* *Escherichia coli* and to identify variants with different aggregation propensity<sup>[18,19]</sup> and toxicity.<sup>[1]</sup> In mammalian cells, an eGFP folding sensor of SOD1 is used to identify mutants with distinct aggregation propensities and increased toxicity.<sup>[20]</sup> Firefly luciferase mutants fused to EGFP have also been used as aggregation sensors in both cells and in animal models, as *C. elegans*.<sup>[21]</sup> Also, Htt-GFP sensors are used to study the impact of expanded polyglutamine (PolyQ) chains on protein aggregation and cell viability, which is relevant to characterize HD.<sup>[22]</sup> More recently, a fluorogenic aggregation prone Halo-tag mutant was developed and is a valuable tool to evaluate drug-induced proteome stress.<sup>[23]</sup>

Although valuable, most of the available protein aggregation sensors are limited to monitor specific proteins. With this in mind, we have developed a protein aggregation sensor that can be used to monitor general protein aggregation in human cells and we have established a stable cell line to test it in multiple physiological conditions. For this, we took advantage of the observation that the small heat shock protein 27 (HSP27), also

M. Pereira, D. Tomé, A. S. Domingues, Dr. A. S. Varanda, C. Paulo, Prof. M. A. S. Santos, Dr. A. R. Soares  
iBiMED – Institute of Biomedicine  
Department of Medical Sciences  
University of Aveiro  
3810-193 Aveiro, Portugal  
E-mail: ana.r.soares@ua.pt

 The ORCID identification number(s) for the author(s) of this article can be found under <https://doi.org/10.1002/biot.201700676>.

See accompanying commentary by Yu Liu and Xin Zhang, <https://doi.org/10.1002/biot.201800039>

© 2018 The Authors. Biotechnology Journal Published by Wiley-VCH Verlag GmbH & Co. KGaA, Weinheim. This is an open access article under the terms of the Creative Commons Attribution License, which permits use, distribution and reproduction in any medium, provided the original work is properly cited.

DOI: 10.1002/biot.201700676

known as HSPB1, is efficiently recruited by misfolded proteins. HSP27 binds to misfolded proteins forming a chaperone-substrate complex that permits refolding by larger ATP-dependent chaperones, namely HSP70 and HSP90 or directing proteins for degradation.<sup>[24]</sup> Therefore, we hypothesized that HSP27 could be used to monitor protein misfolding and protein aggregation in different physiological conditions and pathologies.

Here we show the development of a human HSP27:GFP sensor and a HeLa cell line expressing it in a stable manner. We demonstrate that this sensor is a valuable tool to identify different protein misfolding/aggregation promoting conditions and can be used in fluorescence-based genetic screens to identify novel therapeutic targets and drug candidates that modulate protein aggregation.

## 2. Experimental Section

### 2.1. Protein Aggregation Sensor

The human *HSP27* promoter and coding region without the stop codon were amplified from genomic DNA (gDNA) obtained from HeLa cells. gDNA was isolated from  $10^6$  cells using the NZY tissue gDNA isolation kit from NZYTech, following the manufacturer's protocol. The *HSP27* promoter and coding region were amplified by PCR, using Pfu DNA polymerase. Amplified DNA was cloned at the MluI and XhoI sites of the pcDNA3.1(-) vector (forward primer: 5'-CGACGCGTGTG-TATGCCCAAC-3'; reverse primer: 5'-CCGCTCGAGCT TGGCGGCAGTCTC-3'). Ligation of the *HSP27* insert was performed overnight and JM109 competent cells were transformed with the plasmid. Clones were replated and subjected to PCR to confirm the *HSP27* insertion.

eGFP was amplified from the pCS2 plasmid and cloned at XhoI and HindIII sites of the pcDNA3.1(-)HSP27, originating the pcDNA3.1(-)HSP27:GFP fusion vector (forward primer: 5'-CCGCTCGAGATGGTGAGCAA-3', reverse primer: 5'-CCCAA GCTTTTACTTGTACAGCT-3'). Positive colonies were selected after PCR amplification and confirmed by Sanger sequencing.

### 2.2. Cell Transfection

HeLa cells were cultured in Dulbecco's modified Eagle's medium (DMEM, Gibco), supplemented with 10% fetal bovine serum (FBS, Sigma), 1% antibiotics (Penicillin/Streptomycin, Gibco) and maintained in an incubator under 5% CO<sub>2</sub>/95% air at 37 °C. Cells were transfected with the pcDNA 3.1(-):GFP vector or the pcDNA3.1(-)HSP27:GFP vector. HeLa cells were plated in 1 mL of DMEM complete medium at a density of  $2 \times 10^5$  cells/mL in 6 well plates 24 h prior to transfection. Complete medium was changed to medium without antibiotics 1 h prior to transfection. Transfection complexes were prepared using Lipofectamin<sup>®</sup> 2000 following the manufacturer's instructions. Briefly, Lipofectamin<sup>®</sup> 2000 was incubated with Opti-MEM for 5 min at room temperature. This mixture was incubated with 1 µg of the corresponding plasmid for 20 min at 37 °C. After incubation, the transfection mix was added to cells and incubated at 37 °C. Transfection medium was changed

to complete medium 7 h after transfection and cells were allowed to grow for 72 h before being used for further experiments. Cells transfected with Lipofectamine<sup>®</sup> 2000 only were used as controls. Expression of HSP27:GFP fusion was confirmed by PCR amplification and Sanger sequencing. 5'-AAGCTGACCCT-GAAGTTCATCTGC-3' and 5'-TTACTTGTACAGCTCGTCCA-3' oligonucleotides were used to amplify GFP. 5'-CGGAAATA-CACGTGAGTCCT-3' and 5'-TTACTTGTACAGCTCGTCCA-3' oligonucleotides were used to amplify *HSP27:GFP* fusion by PCR.

### 2.3. Stable Cell Line Generation

Stable cell lines were selected using G418. After transfection, cells were allowed to grow for 72 h. After this period, the medium was changed for fresh medium containing 800 µg mL<sup>-1</sup> of G418. To generate monoclonal cell lines, the polyclonal cell line cultivated in the presence of 800 µg mL<sup>-1</sup> G418 was plated in 96 well plates at a 10 cells/mL density in 100 µL medium. Medium with 800 µg mL<sup>-1</sup> G418 was changed every 3 days and only wells containing one clone were expanded, originating HeLa HSP27:GFP monoclonal stable cell lines.

### 2.4. Reporter Assay

HeLa-HSP27:GFP cells were plated at a  $2 \times 10^5$  cells/mL density in 6 well plates and incubated for 24 h. Cells were then incubated with different stress agents: 5 µM of MG132 (Sigma-Aldrich) for 18 h, 500 nM Arsenite (Sigma-Aldrich), for 30 min and 15 µM of Aβ-amyloid 1-42 (GenicBio Ltd.) for 3 h. After the incubation period, cells were washed with 1xPBS and either collected for protein extraction and subsequent Western blot analysis or fixed in 4% PFA.

### 2.5. HSP27 Immunofluorescence (IF)

Fixed cells were permeabilized with 0.1% Triton X-100 for 15 min. After blocking with Blocking solution (1% BSA, glycine in PBS-T) for 30 min, coverslips were incubated with a 1:100 dilution of anti-mouse HSP27 monoclonal antibody (Stress-Marq) overnight at 4 °C. After incubation, cells were washed with PBS and incubated with Alexa-Fluor 568-conjugated goat anti-mouse IgG antibody at a 1:200 dilution at room temperature for 2 h. Coverslips were incubated with 100 ng mL<sup>-1</sup> DAPI solution for 15 min, washed with PBS, mounted in Vectashield, and visualized in a Zeiss AxioImager M1 epifluorescence microscope using GFP, DAPI, and RFP filters. Images were acquired using the Zeiss AxioVision software.

### 2.6. Statistical Analysis

Data were analyzed using GraphPad Prism. The differences between control and conditioned cells were assessed using a Student's unpaired *t*-test with post-test Dunnett's Multiple Comparison Test. In all cases, *p*-values <0.05 were considered statistically significant.

### 3. Results and Discussion

#### 3.1. Establishment of a Stable Cell Line Expressing HSP27: GFP Protein Aggregation Sensor

We have previously constructed a chimeric HSPB1:mcherry reporter sensor that successfully detects the production of

protein aggregates in zebrafish.<sup>[25]</sup> However, this sensor is transient and zebrafish specific. In order to identify misfolding conditions in human cells, we have developed now a human specific HSP27:GFP chimeric sensor (Figure 1A).

To construct the human HSP27:GFP chimeric protein, the HSP27 coding region without its stop codon and 5' flanking

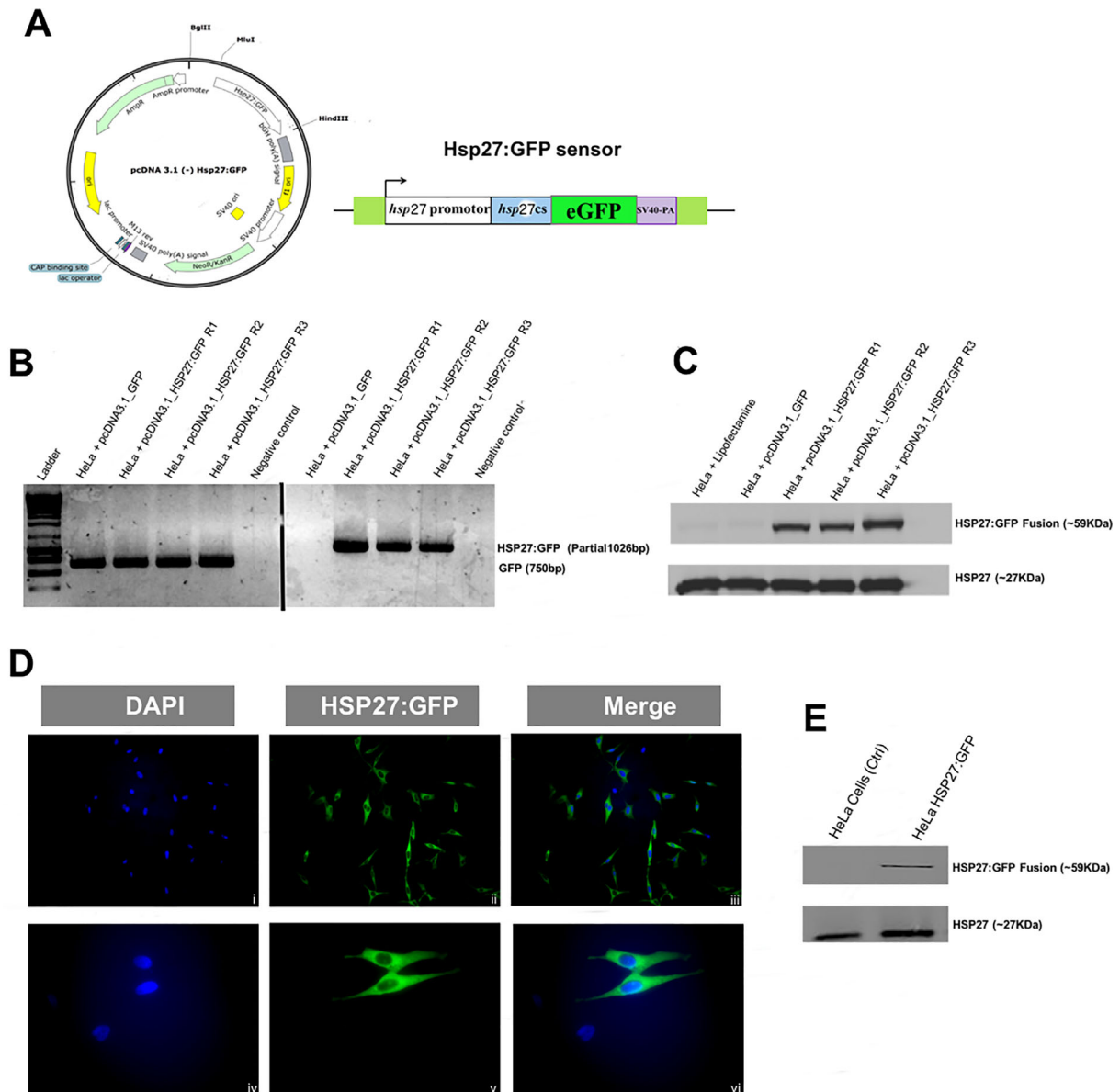


**Figure 1.** HSP27:GFP cloning and establishment of a HeLa cell line expressing the HSP27:GFP sensor. A) Graphical representation of the pcDNA 3.1(-) HSP27:GFP vector. The human HSP27 promoter and coding sequence (cs) were cloned between the MluI and XhoI restriction sites. GFP was fused to the 3' end of HSP27 coding sequence without the stop codon, between the XhoI and HindIII restriction sites, originating the HSP27:GFP sensor. B) PCR amplification of GFP and HSP27:GFP fusion after transfection. GFP (≈750 bp) and the HSP27:GFP fusion (≈1026 bp) were amplified by PCR. HSP27:GFP gene was only detected in cells transfected with the pcDNA3.1(-)HSP27:GFP vector. C) HSP27 western blotting. HSP27 was detected as a 27 kDa band in all samples tested. The HSP27:GFP fusion was only detected in cells transfected with the pcDNA3.1(-):HSP27:GFP vector as a 59 kDa band. D) Fluorescence microscopy. Transfected cells were fixed and their nuclei stained with DAPI (i and iv). Cells were observed under a Zeiss AxioImager epifluorescence microscope using a 20× objective (i–iii) and a 63× objective (iv–vi). Efficiently transfected cells exhibited green fluorescence. E) Expression of HSP27:GFP chimeric protein in stable HeLa HSP27:GFP cell line. Expression of both HSP27 and the HSP27:GFP fusion was detected in the monoclonal HeLa HSP27:GFP stable cell line after G418 selection and clone expansion, whereas the Control HeLa cell line expressed HSP27 only.

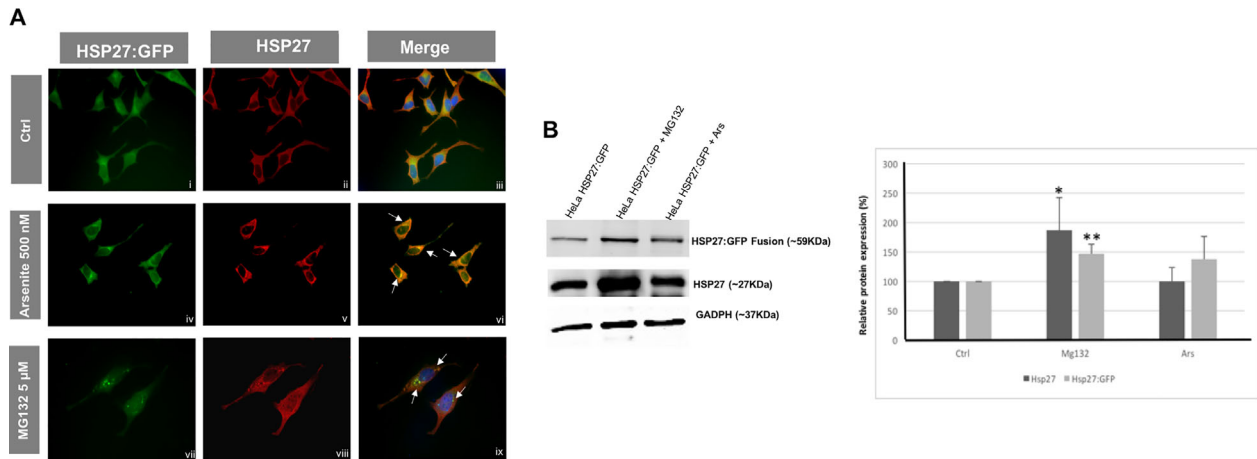


**Figure 2.** HSP27:GFP sensor validation under protein misfolding conditions. A) HSP27 immunofluorescence. Endogenous HSP27 was detected using a primary HSP27 antibody and a secondary Alexa Fluor antibody (ii, v, and viii). HSP27:GFP fusion was detected by direct observation under the epifluorescence microscope using a GFP filter (i, iv, and vii). Images were captured in separate channels (RFP and GFP) and merged using Image J to analyze co-localization between endogenous HSP27 and the fusion protein (iii, vi, and ix). Cells were observed in unstressed conditions (i–iii), after oxidative stress induction by arsenite (iv–vi) and after proteasome inhibition by MG132 (vii–ix). Arrows indicate co-localization of endogenous HSP27 foci with HSP27:GFP foci generated after stress exposure, indicating relocalization of HSP27 to cellular locations where protein misfolding/aggregation occurred. B) HSP27 Western blot of a HeLa HSP27:GFP stable cell line under stress conditions. Both HSP27 and HSP27:GFP fusion expression increased significantly after proteasome inhibition with MG132. GADPH was used as housekeeping gene. Error bars represent the standard deviation of at least three independent replicates. Units are relative to control sample in percentage. Data analysis was performed using Student's unpaired *t*-test (\*  $p < 0.05$ ; \*\*  $p < 0.01$ ).

region containing the promoter were amplified as a  $\approx 1900$  bp product from HeLa cells gDNA preparations.

After amplification of the *HSP27* promoter and coding region, the template was inserted in the pcDNA3.1(–) vector. The *HSP27* promoter replaced the plasmid CMV ubiquitous promoter to prevent constitutive expression of the sensor. JM109 cells were transformed with the resulting plasmid and positive clones containing the pcDNA3.1(–):*HSP27* vector were selected and used for subsequent GFP cloning to originate the pcDNA 3.1(–):*HSP27:GFP* vector. In parallel, GFP was cloned in the original pcDNA3.1(–), originating the pcDNA3.1(–):GFP vector. Positive clones of both vectors were identified by PCR and validated by Sanger sequencing.

To generate a stable cell line expressing the HSP27:GFP chimeric protein, HeLa cells were transfected with the pcDNA 3.1(–):*HSP27:GFP* vector, using Lipofectamine<sup>®</sup> 2000 as the transfection reagent. HeLa cells transfected with Lipofectamine<sup>®</sup> only and HeLa cells transfected with the pcDNA3.1(–):GFP vector were used as controls. As expected, GFP was PCR amplified from all cells transfected with either the pcDNA3.1(–):GFP vector and the pcDNA 3.1(–):*HSP27:GFP* vector, as a  $\approx 750$  bp DNA fragment (Figure 1B). The *HSP27:GFP* fusion could only be amplified from cells transfected with the pcDNA3.1(–):*HSP27:GFP* vector (Figure 1B), indicating that these cells were efficiently transfected with the chimeric sensor.

To confirm that the HSP27:GFP sensor protein was expressed after transfection, Western blotting using a HSP27 antibody was performed (Figure 1C). As HSP27 is constitutively expressed, it was detected by Western blotting in all cell lines tested, namely HeLa cells transfected with Lipofectamine<sup>®</sup> only, HeLa cells transfected with pcDNA3.1(–):GFP and all the replicates transfected with the pcDNA3.1(–):*HSP27:GFP* sensor. An extra

band of  $\approx 59$  kDa corresponding to the HSP27:GFP fusion was only detected in cells transfected with pcDNA3.1(–):*HSP27:GFP*, confirming that the chimeric protein was expressed after transfection in HeLa cells. To further confirm the fluorescent sensor expression, cells were fixed and analyzed by epifluorescence microscopy after transfection (Figure 1D). Nuclei were stained with DAPI (Figure 1D i and iv). Cells efficiently transfected and expressing the sensor exhibited GFP fluorescence (Figure 1D ii, iii, v, and vi).

After transfection confirmation, stable, monoclonal HeLa cell lines expressing HSP27:GFP fusion, named HeLa HSP27:GFP, were established by G418 selection. Expression of the chimeric protein in the stable clones was confirmed by Western blotting (Figure 1E).

### 3.2. HSP27:GFP Sensor Validation as a Protein Misfolding Sensor

After stable cell line generation, the ability of the sensor to be used as a general protein aggregation reporter was evaluated. Monoclonal HeLa HSP27:GFP cells were exposed to different proteome stressors to verify if relocalization of fluorescence to foci occurred – an indicative of the functionality of the fluorescence sensor. HSP27 IF was also performed to analyze the co-localization between HSP27 and the fluorescent chimeric protein (Figure 2A).

Unstressed cells showed even distribution of GFP throughout the cytoplasm, which was also in accordance with HSP27 expression observed by IF (Figure 2A i–iii).

Cells exposed to Arsenite, a known oxidative stress inducer that elicits the cellular stress response, by translation initiation inhibition and formation of stress granules (SGs) [26] displayed



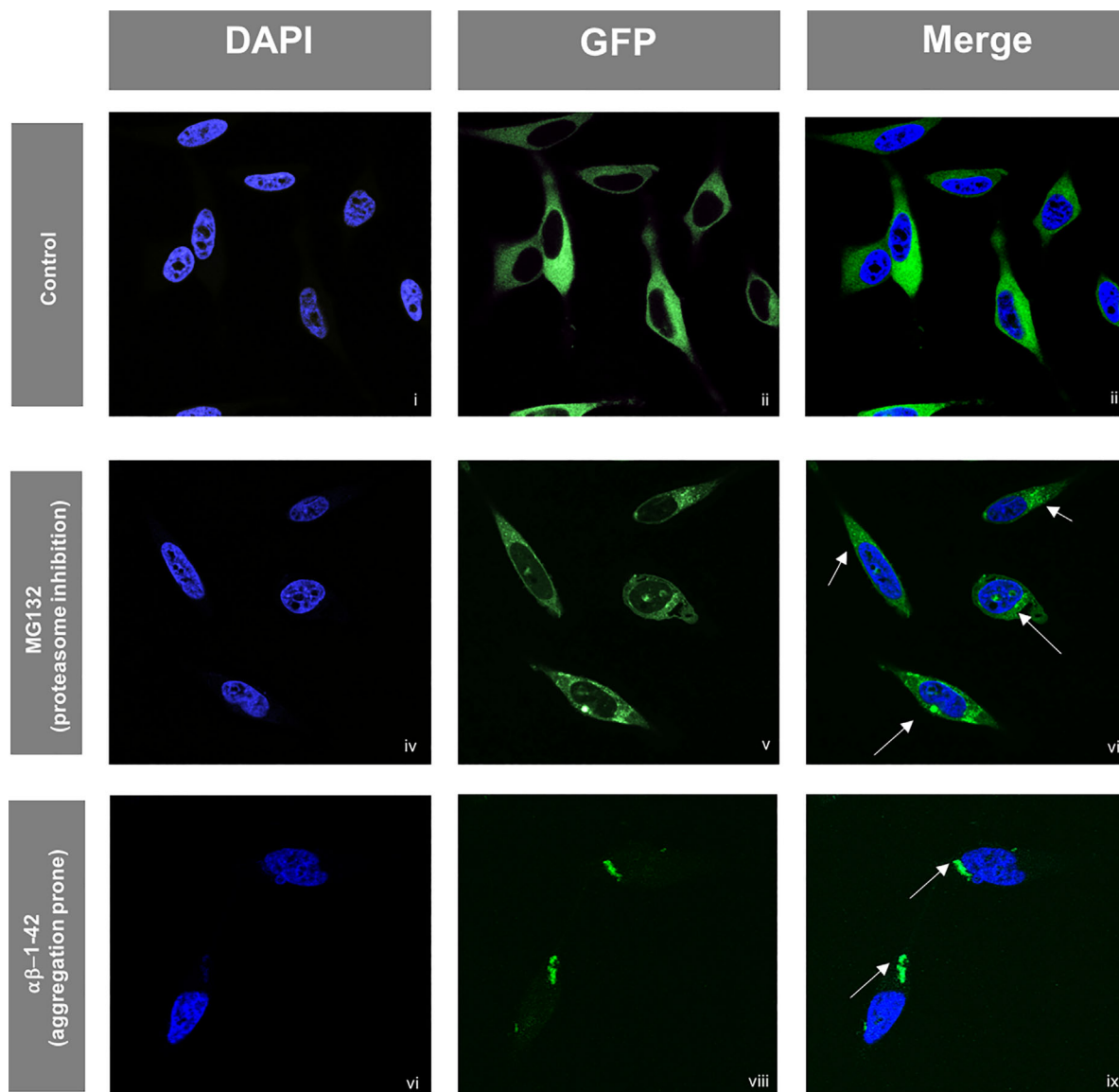


**Figure 3.** HSP27:GFP detects general protein aggregation. Confocal microscopy. HeLa HSP27:GFP cells were fixed, the nuclei stained with DAPI and observed under a Zeiss Confocal microscope in control conditions (i–iii), after proteasome inhibition (iv–vi) and after incubation with an aggregation prone amyloid peptide ( $\alpha\beta$ -1-42) (vii–ix). Images were captured in separate channels using different lasers (Diode for DAPI and Argon for GFP detection) and merged using Image J. Arrows indicate the formation of HSP27:GFP foci after stress exposure, indicating that protein misfolding/aggregation was occurring.

discrete HSP27:GFP foci which co-localized with HSP27 foci, in particular near and inside the nucleus (Figure 2A iv–vi). Formation of foci was expected after exposure to Arsenite, as recent data indicate that misfolded proteins also accumulate in SGs in human cells. For example, ALS-variants of SOD-1 have been found accumulated in SGs that also contain chaperones, including HSP27.<sup>[27]</sup> However, SGs induced by Arsenite are not greatly enriched in HSP27 and are highly dynamic,<sup>[28]</sup> which may explain the detection of only discrete foci. A similar distribution of SGs after Arsenite treatment was observed in a previous study using HeLa cells and the same exposure conditions, corroborating our data.<sup>[29]</sup>

Cells were also exposed to MG132, a potent proteasome inhibitor, to induce the accumulation of aggregated proteins in

cells. This includes accumulation of misfolded and aberrant proteins, that can constitute up to a third of newly synthesized polypeptides. This elicits, among others, the expression of heat shock proteins, including HSP27.<sup>[30]</sup> Our data showed formation of HSP27:GFP foci after proteasome inhibition. This was accompanied by the detection of Hsp27 foci by IF that co-localized with HSP27:GFP foci (Figure 2A vii–ix), demonstrating that HSP27 was recruited to the misfolded proteins accumulating in the cytoplasm. Upon transient transfection of a Hsp27-GFP protein in HEK293T cells, cells treated with a proteasome destabilizer also exhibited the formation of fluorescence puncta,<sup>[23]</sup> similarly to our observations, confirming that Hsp27 is a global aggregation sensor at the cellular level. In addition to this, western blot analysis showed that both

endogenous HSP27 and the HSP27:GFP sensor expression significantly increased after proteasome inhibition (Figure 2B).

### 3.3. HSP27:GFP Sensor Detects a Wide Spectrum of Aggregated Proteins

To confirm that our protein aggregation sensor could be used to detect protein aggregates belonging to the amyloid class, HeLa HSP27:GFP cells were incubated with a synthetic A $\beta$ -amyloid 1-42. This peptide mimics one of the major components of amyloid plaques that accumulate in AD patient's neurons. After incubation, cells were observed by confocal microscopy and compared with unstressed cells and cells exposed to the proteasome inhibitor MG132 (Figure 3). Similarly to what was observed in Figure 2, unstressed cells expressed HSP27:GFP homogeneously in the cytoplasm (Figure 3i–iii). After proteasome inhibition, numerous fluorescent foci were detected in different cytoplasmic locations and also in the nucleus, confirming that the fluorescent sensor detected aberrant proteins that accumulated in cells due to a decrease in protein degradation (Figure 3iv–vi). It is possible that the foci detected in the nuclear region correspond to nucleolar inclusions that accumulate ubiquitin, components of the ubiquitin-proteasome system and proteins associated with neurodegenerative diseases, namely Ataxin-1 and Malin or nuclear transient SGs that contain stress response proteins, including heat shock proteins,<sup>[31]</sup> as these structures have been identified after proteasome inhibition with MG132.<sup>[32]</sup> After incubation and internalization of the synthetic A $\beta$ -amyloid 1-42 peptide, HeLa HSP27:GFP cells showed large fluorescent foci, indicating that the sensor was able to detect intracellular amyloids (Figure 3vi, vii, ix). These observations were confirmed by comparing the protein insoluble fractions from control cells, cells exposed to MG132 and cells exposed to the A $\beta$ -amyloid 1-42 peptide. After exposure to both MG132 and A $\beta$ -amyloid 1-42 peptide there was an increase in insoluble proteins (Appendix and Figure S1A, Supporting Information). To further confirm that the fluorescence sensor detects aggregated amyloids, we have performed a Western blot using an anti- $\beta$ -amyloid (B-4) antibody. As expected, a 4 kDa band, corresponding to the A $\beta$ -amyloid 1-42 peptide was only detected in cells incubated with the synthetic peptide. Moreover, blotting of the insoluble fraction showed that this peptide was indeed insoluble (Appendix Figure S1B, Supporting Information).

Additionally, we used a commercial kit of aggresome detection (Proteostat) that detects aggresome-like inclusion bodies in cells. As expected, unstressed HeLa HSP27:GFP cells showed a basal Proteostat signal only, indicating that the level of aggresomes was very low, which is supported by the homogeneous distribution of the HSP27:GFP sensor in the cell's cytoplasm (Appendix Figure S2i–iv, Supporting Information). After Arsenite exposure, discrete HSP27:GFP foci formed, but only a fraction of cells were Proteostat positive. Similar observations were made after MG132 exposure (Appendix Figure S2v, vi, viii, ix, Supporting Information), indicating that our sensor was more effective in detecting different misfolding occurrences. But, there was strong co-localization of the HSP27:GFP and Proteostat signals after incubation with A $\beta$ -amyloid 1-42 peptide. This was expected as Proteostat detects intracellular amyloid-like deposits with high specificity.<sup>[33]</sup>

## 4. Conclusion

The objective of this work was to develop a HSP27:GFP sensor to detect protein misfolding and protein aggregation, independently of its nature and without the need of additional IF or immunocytochemistry. Most protein aggregates are amyloids, but other classes of proteins also aggregate in specific conditions and may escape detection with existing methods. Our results show that our sensor detects general protein aggregation in an easy manner and has advantages relatively to the available protein-aggregation reporters.

Our sensor is a valuable tool for the development of fluorescence-based screens to identify both genes that affect proteostasis and chemical compounds that lead to protein destabilization. Our stable cell line expressing the fluorescent protein misfolding sensor, allows performing experiments where cellular conditions can be manipulated and observed in real time, representing a valuable asset to understand proteome stability dynamics. Since different human stable cell lines can be established using the HSP27:GFP sensor, it is an important new tool to identify modulators of proteostasis and, consequently, therapeutic targets that can be applied to several protein conformational disorders.

## Abbreviations

$\alpha$ -syn,  $\alpha$ -synuclein; A $\beta$ , amyloid beta; AD, Alzheimer's disease; ALS, amyotrophic lateral sclerosis; ARD, age-related diseases; GFP, green fluorescence protein; HD, Huntington's disease; HSP27, heat shock protein 27; Htt, Huntingtin; PD, Parkinson's disease; SOD-1, superoxide dismutase 1.

## Supporting Information

Supporting Information is available from the Wiley Online Library or from the author.

## Acknowledgments

We acknowledge the Portuguese Foundation for Science and Technology (FCT), POCH, FEDER, and COMPETE2020 for funding, through the grants SFRH/BPD/77528/2011, PTDC/BIM-MEC/1719/2014, PTDC/BEX-BCM/2121/2014, and UID/BIM/04501/2013.

## Conflict of Interest

The authors declare no commercial or financial conflict of interest.

## Keywords

fluorescence sensor assay, GFP, HSP27, human cells, protein aggregation

Received: October 30, 2017

Revised: December 19, 2017

Published online:

[1] V. H. Finder, R. Glockshuber, *Neurodegener. Dis.* **2007**, *4*, 13.

- [2] B. Nizynski, W. Dzwolak, K. Nieznanski, *Protein Sci.* **2017**, 26, 2126.
- [3] F. Chiti, C. M. Dobson, *Annu. Rev. Biochem.* **2017**, 86, 27.
- [4] F. U. Hartl, *Annu. Rev. Biochem.* **2017**, 86, 21.
- [5] M. Zhu, H. S. Patel, S. Han, *Biochim. Biophys. Acta – Gen. Subj.* **2017**, 1861, 1759.
- [6] A. Vandersteen, E. Hubin, R. Sarroukh, G. De Baets, J. Schymkowitz, F. Rousseau, V. Subramaniam, V. Raussens, H. Wenschuh, D. Wildemann, K. Broersen, *FEBS Lett.* **2012**, 586, 4088.
- [7] D. W. Dickson, *Parkinsonism Relat. Disord.* **2017**, 46, S30.
- [8] M. Arrasate, S. Finkbeiner, *Exp. Neurol.* **2012**, 238, 1.
- [9] A. M. Blokhuis, E. J. N. Groen, M. Koppers, L. H. van den Berg, R. J. Pasterkamp, *Acta Neuropathol.* **2013**, 125, 777.
- [10] D. H. Perlmutter, G. A. Silverman, *Cold Spring Harb. Perspect. Biol.* **2011**, 3, pii:a005801.
- [11] D. C. David, N. Ollikainen, J. C. Trinidad, M. P. Cary, A. C. Burlingame, C. Kenyon, *PLoS Biol.* **2010**, 8, e1000450.
- [12] D. M. Walther, P. Kasturi, M. Zheng, S. Pinkert, G. Vecchi, P. Ciryam, R. I. Morimoto, C. Dobson, M. Vendruscolo, M. Mann, F. U. Hartl, *Cell* **2015**, 161, 919.
- [13] S. Ayyadevara, F. Mercanti, X. Wang, S. G. Mackintosh, A. J. Tackett, S. V. Prayaga, F. Romeo, R. J. Shmookler Reis, J. L. Mehta, *Hypertension (Dallas, Tex. 1979)* **2016**, 67, 1006.
- [14] A. Elobeid, S. Libard, M. Leino, S. N. Popova, I. Alafuzoff, *J. Neuropathol. Exp. Neurol.* **2016**, 75, 316.
- [15] D. Wang, Y. Ha, J. Gu, Q. Li, L. Zhang, P. Yang, *Adv. Mater.* **2016**, 28, 7414.
- [16] F. Tao, Q. Han, K. Liu, P. Yang, *Angew. Chemie – Int. Ed.* **2017**, 56, 13440.
- [17] S. Gregoire, J. Irwin, I. Kwon, *Korean J. Chem. Eng.* **2012**, 29, 693.
- [18] W. Kim, M. H. Hecht, *J. Biol. Chem.* **2005**, 280, 35069.
- [19] W. Kim, M. H. Hecht, *J. Mol. Biol.* **2008**, 377, 565.
- [20] S. Gregoire, I. Kwon, *Biotechnol. J.* **2012**, 7, 1297.
- [21] R. Gupta, P. Kasturi, A. Bracher, C. Loew, M. Zheng, A. Villella, D. Garza, F. U. Hartl, S. Raychaudhuri, *Nat. Methods* **2011**, 8, 879.
- [22] P. Lajoie, E. L. Snapp, S. Bekiranov, B. Giepmans, A. Palmer, *PLoS ONE* **2010**, 5, e15245.
- [23] Y. Liu, M. Fares, N. P. Dunham, Z. Gao, K. Miao, X. Jiang, S. S. Bollinger, A. K. Boal, X. Zhang, *Angew. Chemie Int. Ed.* **2017**, 56, 8672.
- [24] A. Strauch, M. Haslbeck, *Essays Biochem.* **2016**, 60, 163.
- [25] M. Reverendo, A. R. Soares, P. M. Pereira, L. Carreto, V. Ferreira, E. Gatti, P. Pierre, G.R. Moura, M. A. Santos, *RNA Biol.* **2014**, 11, 1199.
- [26] E. K. Schmidt, G. Clavarino, M. Ceppi, P. Pierre, *Nat. Methods* **2009**, 6, 275.
- [27] D. Mateju, T. M. Franzmann, A. Patel, A. Kopach, E. E. Boczek, S. Maharana, H. O. Lee, S. Carra, A. A. Hyman, S. Alberti, *EMBO J.* **2017**, 36, 1669.
- [28] N. Kedersha, G. Stoecklin, M. Ayodele, P. Yacono, J. Lykke-Andersen, M. J. Fritzler, D. Scheuner, R. J. Kaufman, D. E. Golan, P. Anderson, *J. Cell Biol.* **2005**, 169, 871.
- [29] K. Fujimura, J. Katahira, F. Kano, Y. Yoneda, M. Murata, *Biochim. Biophys. Acta – Mol. Cell Res.* **2009**, 1793, 1728.
- [30] A. F. Kisselev, A. L. Goldberg, *Chem. Biol.* **2001**, 8, 739.
- [31] L. Latonen, *BioEssays* **2011**, 33, 386.
- [32] L. Latonen, H. M. Moore, B. Bai, S. Jäämaa, M. Laiho, *Oncogene* **2011**, 30, 790.
- [33] S. Navarro, S. Ventura, *Biotechnol. J.* **2014**, 9, 1259.